The Behaviour of Populations in a Rapidly Expanding Plasma Flow

Michio Nishida *

Stoßwellenlabor, Institut für Luft- und Raumfahrt, Technische Hochschule Aachen

(Z. Naturforsch. **30 a**, 1563–1571 [1975]; received August 30, 1975)

The distributions of populations of helium atoms in a source flow expansion were calculated for the two different conditions $T_e=7500$ K, $N_e=10^{14}$ cm^{-3} and $T_e=5000$ K, $N_e=10^{13}$ cm^{-3}. The populations in the levels higher than $n=20$ were taken to be in locally thermal equilibrium with the electrons. The steady state consideration was applied to the populations of the levels from $n=7$ to $n=19$. For the levels lower than $n=6$ the expansion flow term was included. The results show that the calculated population densities of the lower levels deviate greatly from those estimated from the steady state consideration.

I. Introduction

Recently considerable interest was drawn to electronic nonequilibrium phenomena in plasma flows. An electronic nonequilibrium state is such that the excited electronic levels of the atoms in a plasma are not populated according to the Boltzmann relation. Such a state occurs in general in a rapidly expanding plasma flow. In this paper the nonequilibrium among the populations of excited levels of helium in a freejet expansion flow is investigated and the behaviour of the populations is represented. The study of such a behaviour is interesting since it is related to the following topics: The first topic is the problem of electron energy transfer due to collisions between electrons and excited atoms. The change of the electron temperature is partly dependent on the energies incoming to and outgoing from the electron gas due to collisional transitions between excited levels. In particular the transitions between lower levels contribute to the electron energy transfer as much as ionization-recombination does. Since in a low-density plasma or a rapidly expanding plasma flow lower excited levels are not populated according to the Boltzmann relation, one must solve the population continuity equation as well as the electron energy equation in order to determine the behaviour of the electron temperature. A second topic is population inversion which may lead to a plasma dynamic laser. If an expansion can be made sufficiently rapid to reduce populations, the populations will then be governed principally by radiative decay. The population of an excited level which has a shorter radiative lifetime than an upper level can decay by emission more rapidly than that of the upper level. An inversion between these two levels then becomes feasible. Hoffmann and Bohn [1, 2] measured the axial and radial distributions of the population densities of hydrogen atoms in a hydrogen-helium expansion flow and observed the population inversion between the principal quantum numbers $n=5$ and $n=3$. They concluded that it was possible to realize the population inversion by a plasma dynamic method. A third topic is the diagnosis of the plasma by means of spectroscopic technique. In most cases this technique is based on the assumption of a Boltzmann distribution among the levels. Therefore any deviation of the population from the Boltzmann distribution would affect the spectroscopic measurements.

Concerning the above-mentioned problems some investigations of electronic nonequilibrium in an expanding plasma flow have been made [1–6]. Bowen and Park [3] made a computer study of electronic nonequilibrium in recombining nitrogen plasma flows starting from equilibrium in the settling chamber. They solved a system of linear equations for the population densities coupled with the flow equations. Park [4, 5] theoretically and experimentally studied the population distributions of excited nitrogen atoms in the nozzle flow of a nitrogen-hydrogen plasma. His theoretical prediction was confirmed in that the electronic excitation temperatures of hydrogen and the ^{3}P state of nitrogen were higher than the electron temperature. However the excitation temperature of the ^{1}D core state was in agreement with the calculated electron temperature. Experimental and theoretical investigations of electronic nonequilibrium among the populations of the excited levels of potassium which was injected into an argon-helium plasma flow passing through a nozzle were made by McGregor and Mitchner [6]. It was shown that the recombined electrons passing through the energy level structure of potassium formed the basis of the electronic nonequilibrium.

* On leave from Department of Aeronautical Engineering, Kyoto University, Kyoto, Japan.

In the analytical part of the aforementioned works the populations of the excited levels were determined by solving the system of linear algebraic equations for the net rate of appearance of excited atoms, under the assumption that the flow time of the gas through the nozzle was large compared with the relaxation time for the excited level. For the case of the present gas of helium the relaxation time for the lower excited levels varies from 10^{-8} sec at the sonic point (electron density: $10^{14}\,\mathrm{cm}^{-3}$) to 10^{-6} sec in the downstream part of the freejet (electron density: $10^{12}\,\mathrm{cm}^{-3}$) while the flow time of the gas is of the order of 10^{-5} sec. Hence a steady state assumption for the populations is not valid in the range of the electron densities which we treat in the present paper.

The present paper treats a partially ionized gas so that the equations to be solved here are the continuity equations for the electrons and populations, and the electron energy equation. These equations are applied to an ionized freejet expansion flow of helium. Such a flow can be easily obtained in a plasma wind tunnel and the present flow conditions are typical for such a wind tunnel. Ashkenas and Sherman [7] showed that the centerline properties of the freejet expansion were very similar to the source flow expansion. Thereafter many theoretical studies of the properties along the freejet centerline have been carried out by using the source flow expansion model. In the present analysis the source flow expansion model will also be used.

II. Rates of Electronic Excitation and De-excitation

In the excited levels of the helium atom singlet and triplet members exist. In the first discussion the singlet and triplet members are separately considered, but in the actual calculations the singlet and triplet levels with equal principal quantum number that is higher than $n=5$ will be considered as one level. Using a collisional-radiative transition model, the net rate of appearance of the helium atoms in the jth level is given by

$$\begin{aligned}\dot{N}_j = &\sum_{s=0}^{\infty} Q(s,j) N_e N_s - \sum_{s=0}^{\infty} Q(j,s) N_e N_j \\ &+ \sum_{p=1}^{\infty} P(p,j) N_e N_p - \sum_{p=1}^{\infty} P(j,p) N_j N_e \\ &+ Q_R(e^-, j) N_e{}^2 - Q_I(j, e^-) N_e N_j \\ &+ \sum_{s=j+1}^{\infty} A(s,j) N_s - \sum_{s=0}^{j-1} A(j,s) N_j\end{aligned} \tag{1}$$

where N_e is the electron density; N_j the population density in the jth excited level of helium, $Q(s,j)$ the collisional rate constant for the transition from the sth level to the jth level, $A(s,j)$ the Einstein A coefficient for a radiative transition from the sth level to the jth level, $Q_R(e^-, j)$ the collisional recombination rate constant to the jth level, $Q_I(j, e^-)$ the collisional ionization rate constant from the jth level. When we are considering N_j as the population density of the singlet level, N_p denotes the population density of the triplet level, and vice versa. P represents the collisional rate constant for the transition between the singlet and triplet levels. In Eq. (1) the transitions due to the collisions between electrons and excited atoms are considered as collisional transitions. In the present temperature range ($T<7500$ K) the excited atom-atom collisions are not important [8].

The collisional transition probability for the excitation from the jth level to kth level integrated over the Maxwellian electron-velocity distribution can be written as

$$N_e Q(j,k) = \int_{E_{j,k}}^{\infty} \frac{dN_e}{dE} v(E)\, \sigma_{j,k}(E)\, dE \tag{2}$$

with

$$\frac{dN_e}{dE} = \left(\frac{8}{\pi m_e}\right)^{\frac{1}{2}} \frac{N_e}{(k T_e)^{3/2}} \frac{E}{v} \exp\left\{-\frac{E}{k T_e}\right\} \tag{3}$$

where $v(E)$ is the velocity of an electron of energy E and $E_{j,k}$ the energy difference between the jth and kth level. T_e is the electron temperature. The cross section for the transition from the jth level to the kth level $\sigma_{j,k}(E)$ is estimated from the modified Thomson formula which was proposed by Kogan et al. [9]

$$\sigma_{j,k}(E) = \begin{cases} \dfrac{\pi e^4}{E}\left(\dfrac{1}{E_{j,k}} - \dfrac{1}{E_{j,k+1}}\right) & \text{for } E \geqq E_{j,k+1}, \\ \dfrac{\pi e^4}{E}\left(\dfrac{1}{E_{j,k}} - \dfrac{1}{E}\right) & \text{for } E_{j,k+1} \geqq E \geqq E_{j,k}. \end{cases} \tag{4}$$

After substituting Eqs. (3) and (4) into Eq. (2) and integrating Eq. (2), we have

$$\begin{aligned}N_e Q(j,k) = &\pi e^4 N_e \left(\frac{8}{\pi m_e}\right)^{\frac{1}{2}} (k T_e)^{-\frac{3}{2}} \\ &\cdot \left[\frac{\exp\{-u_{j,k}\}}{u_{j,k}(u_{j,k}+1)} - \frac{\exp\{-u_{j,k+1}\}}{u_{j,k+1}(u_{j,k+1}+1)}\right]\end{aligned} \tag{5}$$

where $u_{j,k}=E_{j,k}/kT_e$. The collisional transition probability for de-excitation is determined by the principle of detailed balance

$$Q(k,j)=(g_j/g_k)\exp\{u_{j,k}\}\,Q(j,k)\ (j<k)\,. \quad (6)$$

Recently Shirai and Tabei [10] showed that for the helium atom the collisional de-excitation rate constants derived from the modified Thomson's formula agreed well with the measured ones in a range of the principal quantum number from $n=3$ to $n=9$ rather than the deexcitation rate constant derived from the Gryzinski's cross section [11].

The expression of the rate constants for the collisional transition from the singlet to triplet and the inverse transition were proposed by Drawin and Emard [12]. For the excitation transition from the triplet to singlet states, the expression is

$$P^{TS}(j,j)=7.2\times10^{-7}\,j^6\,T_e^{-\frac{1}{2}}\frac{E_1^S-E_1^T}{E_I^H}\exp\left\{-\frac{E_j^S-E_j^T}{kT_e}\right\}(\mathrm{cm^3\,sec^{-1}})\,. \quad (7)$$

For $k>j$, the following expression is also proposed:

$$P^{TS}(j,k)=2.862\times10^{-6}\left(\frac{E_1^S-E_1^T}{E_k^S-E_j^T}\right)^2 T_e^{-\frac{1}{2}}\exp\left\{-\frac{E_k^S-E_j^T}{kT_e}\right\}(\mathrm{cm^3\,sec^{-1}})\,. \quad (8)$$

In Eq. (7) E_I^H represents the ionization energy of hydrogen, the superscript TS the transition from the triplet to the singlet level and the superscripts S and T the singlet and triplet states, respectively. Equation (8) with the superscripts S and T interchanged holds for the collisional excitation transition from the singlet to the triplet state. For the inverse transitions to the above-mentioned transitions one can easily obtain the expression of the rate constants by means of the principle of detailed balance. The collisional ionization rate from the jth level is expressed as $Q_I(j,e^-)N_eN_j$. The rate of the inverse process is obtained by substituting for N_j the equilibrium value from the Saha equation because the two rates must be equal at equilibrium. Therefore, the fifth and sixth terms on the R.H.S. of Eq. (1) are expressed as

$$Q_I(j,e^-)N_eN_{j,E}-Q_I(j,e^-)N_eN_j$$

where $N_{j,E}$ is the equilibrium value of the population density at the jth level. The ionization cross section from the jth level is given by [13]

$$\sigma_{j,I}(E)=\frac{\pi e^4}{E}\left(\frac{1}{E_{j,\infty}}-\frac{1}{E}\right) \quad (9)$$

where $E_{j,\infty}$ is the difference between the ionization energy and the excitation energy of the jth level. Using Eq. (9) for Eq. (2) we can easily obtain the following ionization probability:

$$N_eQ_I(j,\infty)=\pi e^4N_e\left(\frac{8}{\pi m_e}\right)^{\frac{1}{2}}\cdot(kT_e)^{-\frac{3}{2}}\frac{\exp\{-u_{j,\infty}\}}{u_{j,\infty}(u_{j,\infty}+1)}\,. \quad (10)$$

The radiative transition probabilities of the helium atom are given in Ref. [14].

The net rate of the electron production will be obtained by summing $Q_I(j,e^-)N_eN_j-Q_I(j,e^-)N_eN_{j,E}$ over j from $j=0$ to $j=\infty$. For highly excited levels, it may be considered that equilibrium is accomplished so that the summation can be cut off at a certain level n^*, above which the populations are in locally thermal equilibrium. The net rate of the electron production is expressed as

$$\dot N_e=N_e\sum_{j=0}^{n^*}[Q_I^S(j,e^-)(N_j^S-N_{j,E}^S)]+N_e\sum_{j=0}^{n^*}[Q_I^T(j,e^-)(N_j^T-N_{j,E}^T)]\,. \quad (11)$$

The population density in the region of $j\geqq n^*$ is given by the Saha equilibrium equation:

$$N_{j,E}=N_e^2\frac{g_j}{2U_i}\left(\frac{h^2}{2\pi m_e kT_e}\right)^{\frac{3}{2}}\exp\left(\frac{I-\Delta I-E_j}{kT_e}\right) \quad (12)$$

where U_i is the partition function of the ion, h Planck's constant, m_e the electron mass, k the Boltzmann constant, I the ionization energy, and ΔI the lowering of the ionization energy due to electric microfields.

III. Governing Equations for Source Flow Expansion

We are considering a partially ionized gas which can be easily realized in a plasma wind tunnel so that the gas components are atoms (including excited atoms), ions, and electrons. In order to simplify the analysis, we introduce the following assumptions: (1) $N_i=N_e$, (2) $T_i=T_a$, (3) $u_a=u_i=u_e\equiv u$, (4) the degree of ionization $\alpha_e\ll1$, (5) $T_{a\perp}=T_{a\parallel}$ and $T_{e\perp}=T_{e\parallel}$. Since the degree of ionization is negligible compared with unity, the

behaviour of neutral particles is not influenced by the existence of charged particles. Therefore the overall continuity, momentum, and energy equations of the gas of interest are essentially those of the neutral particles. These equations have analytical solutions as a function of Mach number. Since the equations of neutral particles are de-coupled with the equations of the electrons and populations, the governing equations to be solved here are reduced to the continuity equations of the electrons and populations and the electron energy equation. For the source flow expansion, they are written as

Electron continuity:

$$\frac{1}{r^2}\frac{\mathrm{d}}{\mathrm{d}r}(r^2 N_\mathrm{e} u) = \dot{N}_\mathrm{e} . \tag{13}$$

Population continuity:

$$\frac{1}{r^2}\frac{\mathrm{d}}{\mathrm{d}r}(r^2 N_j u) = \dot{N}_j . \tag{14}$$

Electron energy:

$$\tfrac{3}{2} k N_\mathrm{e} u \frac{\mathrm{d}T_\mathrm{e}}{\mathrm{d}r} + N_\mathrm{e} k T_\mathrm{e}\left(\frac{\mathrm{d}u}{\mathrm{d}r} + \frac{2u}{r}\right) = R + L - \tfrac{3}{2} k T_\mathrm{e} \dot{N}_\mathrm{e} \tag{15}$$

where r is the distance from the source. The energy transfer rate due to elastic collisions, R, is expressed as

$$R = 2 N_e m_\mathrm{e} \sum_k \frac{\nu_{ek}}{m_k} [\tfrac{3}{2} k (T_k - T_\mathrm{e})] \tag{16}$$

where ν_{ek} represents the collision frequency for the electron-k-species encounters, which is estimated from

$$\nu_{ek} = \frac{4\pi N_k m_\mathrm{e}}{3 k T_\mathrm{e}} \int f(v) \sigma_{ek}(v) v^5 \, \mathrm{d}v . \tag{17}$$

In the above equation f is the distribution function and σ_{ek} the cross section for the electron-k-species encounters. Using the Coulomb cross section for the electron-ion encounters, the electron-ion collision frequency is of the form [15]

$$\nu_\mathrm{ei} = \frac{8}{3}\left(\frac{\pi}{m_\mathrm{e}}\right)^{\frac{1}{2}} N_\mathrm{e} e^4 \frac{1}{(2 k T_\mathrm{e})^{\frac{3}{2}}} \log_\mathrm{e}\left[\frac{9 k^3 T_\mathrm{e}^3}{4\pi N_\mathrm{e} e^6}\right]. \tag{18}$$

One may assume that an effective scattering cross section for the electron-atom encounters is taken to be constant over the likely range of the electron temperature. In this case the electron-atom collision frequency is given by

$$\nu_\mathrm{ea} = N_\mathrm{a}\left(\frac{8 k T_\mathrm{e}}{\pi m_\mathrm{e}}\right)^{\frac{1}{2}} \sigma_\mathrm{ea} . \tag{19}$$

For the case of the helium atom σ_ea is expressed as, for $T_\mathrm{e} < 10^4$ K

$$\sigma_\mathrm{ea} = (0.946 \log T_\mathrm{e} + 2.99) \times 10^{-16} \ \mathrm{cm}^2 \ (T_\mathrm{e} \text{ in K}) . \tag{20}$$

The energy transfer rate due to inelastic collisions, L, is expressed as

$$\begin{aligned} L = &- \sum_{k=1}^{n^*} \sum_{j=0}^{n^*-1} (E_k^\mathrm{S} - E_j^\mathrm{S}) \ [Q^\mathrm{SS}(j,k) N_j^\mathrm{S} N_\mathrm{e} \\ &\qquad - Q^\mathrm{SS}(k,j) N_k^\mathrm{S} N_\mathrm{e}] \\ &- \sum_{k=1}^{n^*-1} \sum_{j=1}^{n^*-1} (E_k^\mathrm{S} - E_j^\mathrm{T}) \ [P^\mathrm{TS}(j,k) N_j^\mathrm{T} N_\mathrm{e} \\ &\qquad - P^\mathrm{ST}(k,j) N_k^\mathrm{S} N_e] \\ &- \sum_{j=0}^{n^*} (I - E_j^\mathrm{S}) Q_\mathrm{I}^\mathrm{S}(j, \mathrm{e}^-)(N_j^\mathrm{S} - N_{\mathrm{j,E}}^\mathrm{S}) N_\mathrm{e} \\ &- \text{(the above three terms with the superscripts S and T replaced by T and S, respectively)} \end{aligned} \tag{21}$$

The first and second terms on the R.H.S. of Eq. (21) represent the transfer rates of the electron energy due to transitions between the singlet levels and between the singlet and triplet levels, respectively. The third term denotes the net rate of the electron energy transfer due to ionization and recombination. Although many investigations of a partially ionized gas flow have been made, the electron energy transfer due to transitions between excited levels was not taken into account. Instead, $[I + (3/2) k T_\mathrm{e}] \dot{N}_\mathrm{e}$ was considered as the energy transfer by the electrons due inelastic collisions. This consideration is based not only on the assumption that all electrons that are captured by ions into highly excited bound states cascade to the ground level and that the electrons do not stay in any excited level but also on the assumption of the steady state population model. For the case of a partially ionized gas this assumption will break since it is expected that populations in such a plasma are not in local thermal equilibrium. Besides the steady state will not be accomplished for the lower levels in a rapid expansion flow. We must therefore obtain the electron energy transfer rate due to inelastic collisions from the knowledge of the transitions between excited levels of the gas of interest. The following dimensionless quantities are introduced:

$$\begin{aligned}
&\alpha_e = N_e'/N' ,\ \alpha_j = N_j'/N' ,\ N = N'/N^* ,\ u = u'/u^* ,\\
&T_a = T_a'/T_a^* ,\ T_e = T_e'/T_e^* ,\ r = r'/r^* ,\ E = E'/k T_e^* ,\\
&I = I'/k T_e^* ,\ \nu_{ij} = \nu_{ij}' r^*/u^* ,\\
&Q(j,k) = Q'(j,k) r^* N^*/u^* ,\\
&P(j,k) = P'(j,k) r^* N^*/u^* ,\\
&A(k,j) = A'(k,j) r^*/u^* , R = R' r^*/k T_e^* N^* u^* ,\\
&L = L' r^*/k T_e^* N^* u^* .
\end{aligned} \tag{22}$$

The prime has been added to denote dimensional quantities and the asterisk denotes the dimensional value at the sonic point. The electron and population densities are non-dimensionalized by the local value of the neutral density. Using the relation $r^2 N u = 1$, the governing equations in the dimensionless form are expressed as

$$\begin{aligned}
d\alpha_e/dr = {} & r^2 N^2 \alpha_e \sum_{j=0}^{n^*} [(\alpha_j^S - \alpha_{j,E}^S) Q_I^S(j, e^-)] \\
& + r^2 N^2 \alpha_e \sum_{j=0}^{n^*} [(\alpha_j^T - \alpha_{j,E}^T) Q_I^T(j, e^-)] ,
\end{aligned} \tag{23}$$

$$\begin{aligned}
d\alpha_j^S/dr = {} & r^2 N^2 \alpha_e \left[\sum_{s=0}^{\infty} \alpha_s^S Q^{SS}(s,j) - \sum_{s=0}^{\infty} \alpha_j^S Q^{SS}(j,s) \right] \\
& + r^2 N^2 \alpha_e \left[\sum_{p=1}^{\infty} \alpha_p^T P^{TS}(p,j) - \sum_{p=1}^{\infty} \alpha_j^S P^{ST}(j,p) \right] \\
& + r^2 N^2 \alpha_e Q_I^S(j, e^-) \quad (\alpha_{j,E} - \alpha_j) \\
& + r^2 N \left[\sum_{s=j+1}^{\infty} A^{SS}(s,j) \alpha_s^S - \alpha_j^S \sum_{s=0}^{j-1} A^{SS}(j,s) \right] ,
\end{aligned} \tag{24}$$

$$\begin{aligned}
& \tfrac{3}{2} N \alpha_e u \frac{dT_e}{dr} + N \alpha_e T_e \left(\frac{du}{dr} + \frac{2u}{r} \right) \\
& = 3 \frac{m_e}{m_a} N \alpha_e (\nu_{ei} + \nu_{ea}) (T_a/\tau^* - T_e) + H
\end{aligned} \tag{25}$$

where $\tau^* = T_e^*/T_a^*$. Setting $H = L - (3/2) T_e \dot{N}_e$, we have

$$\begin{aligned}
H = {} & - \alpha_e N^2 \sum_{k=1}^{n^*} \sum_{j=0}^{n^*-1} (E_k^S - E_j^S) \\
& \cdot [\alpha_j^S Q^{SS}(j,k) - \alpha_k^S Q^{SS}(k,j)] \\
& - \alpha_e N^2 \sum_{k=1}^{n^*-1} \sum_{j=1}^{n^*-1} (E_k^S - E_j^T) \\
& \cdot [\alpha_j^T P^{TS}(j,k) - \alpha_k^S P^{ST}(k,j)] \\
& - \alpha_e N^2 \sum_{j=0}^{n^*} \left(I - E_j^S + \frac{3}{2} T_e \right) (\alpha_j^S - \alpha_{j,E}^S) Q_I^S(j, e^-) \\
& - \text{(the above three terms with the superscripts S and T replaced by T and S, respectively).}
\end{aligned} \tag{26}$$

Equation (24) with the superscripts S and T replaced by the superscripts T and S, respectively, is used for the triplet-level populations. Introducing a new variable

$$S = \tfrac{3}{2} \log_e T_e + \log_e u + 2 \log_e r \tag{27}$$

then the electron energy equation is rewritten as

$$\frac{dS}{dr} = \frac{3(m_e/m_a)}{u T_e} \left(\frac{T_a}{\tau^*} - T_e \right) (\nu_{ei} + \nu_{ea}) + \frac{H}{N \alpha_e u T_e} . \tag{28}$$

The term of the velocity gradient in the electron energy equation, that becomes infinite at the sonic point, has disappeared by the above procedure so that it is possible to start the numerical integration at the sonic point. The following expression is obtained from Eq. (27) by using the relation $r^2 N u = 1$:

$$T_e = \exp\{\tfrac{2}{3} S\} T_a . \tag{29}$$

Thus, once S and T_a are obtained, one may estimate T_e. The atom temperature, density, and velocity can easily be obtained from the isentropic expansion relations. They are written in terms of the Mach number M as follows:

$$T_a = \left(\frac{2}{\gamma+1} + \frac{\gamma-1}{\gamma+1} M^2 \right)^{-1} , \tag{30}$$

$$N = \left(\frac{2}{\gamma+1} + \frac{\gamma-1}{\gamma+1} M^2 \right)^{-1/(\gamma-1)} , \tag{31}$$

$$u = M \left(\frac{2}{\gamma+1} + \frac{\gamma-1}{\gamma+1} M^2 \right)^{-1/2} \tag{32}$$

where γ is ratio of the specific heat. The non-dimensional distance from the source is related to the Mach number as follows:

$$r^2 = \frac{1}{M} \left(\frac{2}{\gamma+2} + \frac{\gamma-1}{\gamma+1} M^2 \right)^{(\gamma+1)/2(\gamma-1)} . \tag{33}$$

IV. Calculation Procedure

The excited level model of the helium atom to be used here is as follows: For $n \leqq 4$ (n: the principal quantum number) the singlet and triplet levels have been separately treated and especially the 2 s- and 2 p-level have been individually treated because of the large energy difference between them. For $n > 4$ both members have been treated as one level. In the electron temperature and electron density ranges of the present expansion flow the steady state populations have been calculated for the case where both members were separated up to higher levels and the resulting population difference of the corresponding levels of both term ladders was quite negligible. Thus the justification of the above treatment was

confirmed. The groupings of the actual quantum states are shown in Table 1. The populations of

Table 1. Groupings of actual quantum states.

j	Singlet	Triplet
0	$1s^2\,{}^1S$	
1	$2s^1S$	$2s^3S$
2	$2p^1P$	$2p^3P$
3	$3s^1S$, $3d^1D$, $3p^1P$	$3s^3S$, $3d^3D$, $3p^3P$
4	$n=4$	$n=4$
5	$n=5$	
6	$n=6$	
.	.	
.	.	
.	.	

$n \geqq 7$ are considered to have a relaxation time of de-excitation sufficiently smaller than the flow time so that the population continuity equation of the highly excited levels can be reduced to the following algebraic equation:

$$N\alpha_e\left[\sum_{s=0}^{\infty}\alpha_s Q(s,j)-\alpha_j\sum_{s=0}^{\infty}Q(j,s)\right]+N\alpha_e Q_1(j,e^-)\,(\alpha_{j,E}-\alpha_j)+\sum_{s=j+1}^{\infty}A(s,j)\alpha_s-\alpha_j\sum_{s=0}^{j-1}A(j,s)=0 \quad (34)$$

$$(j=7,8,9,\ldots,n^*-1)\,.$$

In the above equation the term corresponding to the second term on the R.H.S. of Eq. (24) has disappeared since for $n \geqq 7$ we consider the singlet and triplet levels with equal principal quantum number as one level. It has been assumed that the levels of $n \geqq 20$ are populated according to Saha equilibrium so that $n = 20$ is taken to be n^*.

In the present calculations the net population rates incoming from the adjacent and next adjacent levels and outgoing to these levels have only been considered since the probabilities of these transitions are by an order of magnitude larger than those from and to other levels.

Except for the transitions from the ^1P to the ground state, the plasma considered here is taken to be optically thin. The effective value of the radiative transition rate from any state of ^1P to the ground state is zero due to radiation trapping.

The steady state condition has been used in order to determine the initial population density at the sonic point since it is expected that the flow time is sufficiently large compared with the relaxation time for all levels upstream of the sonic point.

All calculations have been carried out by using the Runge-Kutta-Gill method, on the digital computer CD 6400 at the Computer Center of the Technische Hochschule Aachen.

V. Calculated Results and Discussions

Figures 1 and 2 show the axial distributions of the population density that were calculated for two initial conditions: Case I: $T_e^* = T_a^* = 7500$ K, $N_e^* = 10^{14}\,\mathrm{cm}^{-3}$, $N_a^* = 10^{16}\,\mathrm{cm}^{-3}$ and Case II: $T_e^* = T_a^* = 5000$ K, $N_e^* = 10^{13}\,\mathrm{cm}^{-3}$, $N_a^* = 10^{16}\,\mathrm{cm}^{-3}$. These conditions correspond to the following stagnation conditions: Case I: $T_{a0} = 10\,000$ K, $N_{a0} = 1.54 \times 10^{16}\,\mathrm{cm}^{-3}$, $p_0 = 15.9$ Torr and Case II: $T_{a0} = 6670$ K, $N_{a0} = 1.54 \times 10^{16}\,\mathrm{cm}^{-3}$, $p_0 = 10.6$ Torr. In these figures the symbols S and T represent the singlet and triplet members, respectively. The Boltzmann plots for these initial conditions are shown in Figure 3. In Case I the levels of $n \geqq 3$ are populated closely to the Saha equilibrium. This case is such that the collisional transitions are dominant not only in higher levels but also in lower levels. In Case II the dominant collisional transitions are confined to higher levels. We call Case I the case of higher electron density and Case II the case of lower elec-

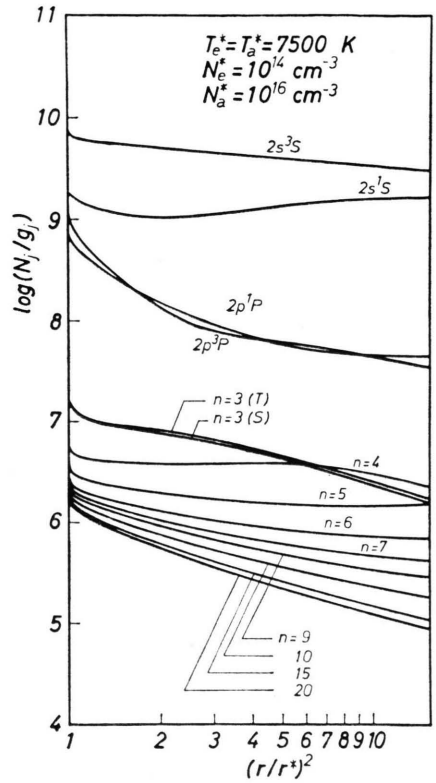

Fig. 1. Axial distributions of population densities for Case I.

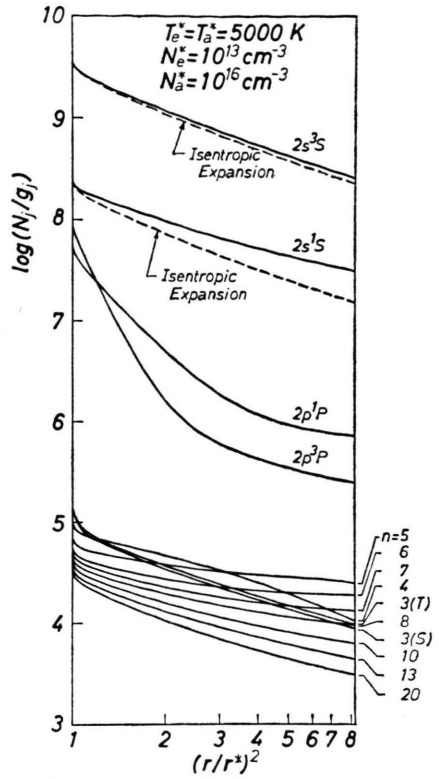

Fig. 2. Axial distributions of population densities for Case II.

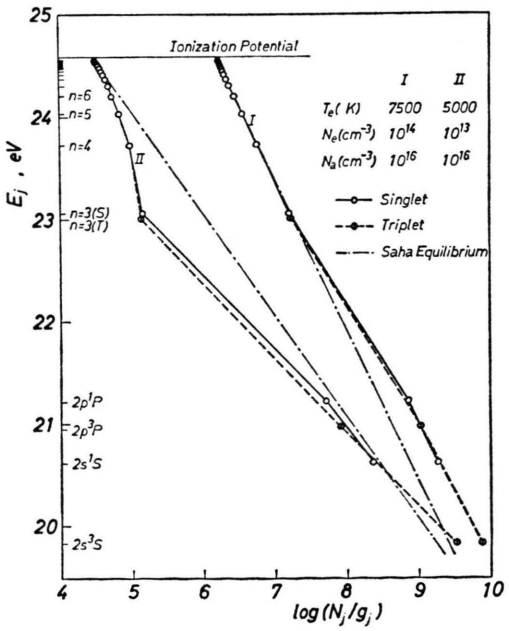

Fig. 3. Boltzmann plots for initial populations.

tron density. The calculations were stopped at $T_e = 800$ K since Eq. (18) is not applicable for lower temperatures. In Figs. 1 and 2 near the sonic point a rapid decreases in the population densities can be seen. This behaviour results from the rapid decrease in the electron density near the sonic point. The behaviour of the population for $n \geqq 4$ is similar in both cases. However there exist significant differences among the behaviours of $2s^3S$, $2s^1S$, $2p^3P$ and $2p^1P$. Such differences may be explained by the following reasoning: In the case of the lower electron density (Fig. 2) the incoming population flux from higher levels to these levels, which is controlled mainly by radiative transitions, is small compared with the case of the higher electron density (Fig. 1). This is because the population density of higher levels is small in the case of the lower electron density. The populations outgoing from $2p^3P$ and $2p^1P$ are controlled by radiative transitions so that this efflux causes a rapid decrease in the population of these two levels. On the other hand the radiative transitions from $2s^3S$ and $2s^1S$ to the ground state are optically forbidden so that the behaviour of these populations approaches the variation due to an isentropic expansion. In Fig. 2 the decrease due to isentropic expansion is also shown. The population distribution of $2s^3S$ is very similar to that due to isentropip expansion while the population of $2p^3P$ decreases more rapidly than that of $2p^1P$. The latter results from the fact that the radiative transition rate from $2p^3P$ is by one order of magnitude larger than that from $2p^1P$. This behaviour cannot be observed in the higher electron density case where the influence of the collision-dominant transitions extends to lower levels. However even in the case of the higher electron densities it is expected that the expansion affects the population behaviour, expecially in lower levels. The comparison of the population densities obtained from the expansion flow calculation and from the steady state model are given in Tables 2 and 3. For the case of the higher electron density (Table 2) the deviations from the steady state population are large for the lowest four levels while for $n \geqq 3$ the deviations become small. For the lower electron density case the deviations extend to levels as high as $n = 10$. Obviously in the expansion flow the exact population densities cannot be obtained from steady state calculations.

Figure 4 shows the deviations of the Boltzmann plots for $n \geqq 3$. At $r/r^* = 1$ (the sonic point) the

Table 2. Comparison between the populations obtained from the expansion flow calculation and from the steady state model. $T_e^*=T_a^*=7500$ K, $N_e^*=10^{14}$ cm^{-3}, $N_a^*=10^{16}$ cm^{-3}, $r/r^*=2.78$, $T_e=1280$ K, $N_e=6.94\times10^{12}$ cm^{-3}.

	N/g from expansion flow calculation	N/g from steady state model
$2s^3S$	3.60×10^9	2.92×10^{11}
$2s^1S$	1.53×10^9	9.12×10^9
$2p^3P$	5.01×10^7	6.11×10^7
$2p^1P$	4.70×10^7	7.05×10^7
$n=3$ (T)	3.14×10^6	3.08×10^6
(S)	2.91×10^6	2.85×10^6
$n=4$ (T)	3.67×10^6	3.60×10^6
(S)	3.41×10^6	3.34×10^6
$n=5$	1.43×10^6	1.38×10^6
$n=6$	7.44×10^5	7.10×10^5
$n=7$	4.97×10^5	4.86×10^5
$n=8$	3.76×10^5	3.71×10^5
$n=9$	3.08×10^5	3.06×10^5
$n=10$	2.66×10^5	2.64×10^5
$n=11$	2.37×10^5	2.36×10^5
$n=12$	2.16×10^5	2.15×10^5
$n=13$	2.00×10^5	1.99×10^5
$n=14$	1.87×10^5	1.87×10^5
$n=15$	1.77×10^5	1.77×10^5
$n=16$	1.69×10^5	1.69×10^5
$n=17$	1.62×10^5	1.62×10^5
$n=18$	1.57×10^5	1.57×10^5
$n=19$	1.52×10^5	1.52×10^5

Table 3. Comparison between the populations obtained from the expansion flow calculation and from the steady state model. $T_e^*=T_a^*=5000$ K, $N_e^*=10^{13}$ cm^{-3}, $N_a^*=10^{16}$ cm^{-3}, $r/r^*=2.41$, $T_e=1030$ K, $N_e=9.38\times10^{11}$ cm^{-3}.

	N/g from expansion flow calculation	N/g from steady state model
$2s^3S$	3.76×10^8	1.02×10^{10}
$2s^1S$	3.99×10^7	4.82×10^8
$2p^3P$	3.15×10^5	2.89×10^5
$2p^1P$	8.53×10^5	8.75×10^5
$n=3$ (T)	1.23×10^4	9.35×10^3
(S)	1.31×10^4	9.99×10^3
$n=4$ (T)	1.68×10^4	1.27×10^4
(S)	1.66×10^4	1.26×10^4
$n=5$	2.79×10^4	2.15×10^4
$n=6$	1.98×10^4	1.41×10^4
$n=7$	1.44×10^4	1.27×10^4
$n=8$	1.09×10^4	1.01×10^4
$n=9$	8.83×10^3	8.47×10^3
$n=10$	7.54×10^3	7.34×10^3
$n=11$	6.67×10^3	6.56×10^3
$n=12$	6.04×10^3	5.97×10^3
$n=13$	5.56×10^3	5.51×10^3
$n=14$	5.19×10^3	5.16×10^3
$n=15$	4.89×10^3	4.87×10^3
$n=16$	4.64×10^3	4.63×10^3
$n=17$	4.44×10^3	4.43×10^3
$n=18$	4.27×10^3	4.26×10^3
$n=19$	4.13×10^3	4.12×10^3

levels are populated closely to equilibrium with the free electrons. The ratio of $N_j/N_{j,E}$ takes the value

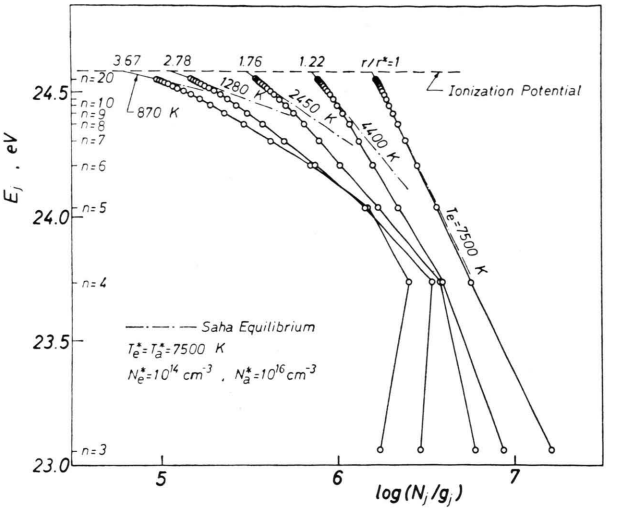

Fig. 4. Deviations of Boltzmann plots for Case I.

of 0.968 even for $n=3$ (singlet). In this figure we can see how the highly excited levels deviate from the equilibrium state. An inversion of the level $n=4$ relative to the level $n=3$ occurs already at $r/r^*=2.78$ ($T_e=1280$ K). This inversion is interesting because of the optically allowed transition from $n=4$ to $n=3$. Inversions occur more strongly in the case of the lower electron density, which is seen in Figure 2.

In the present work the net flux of electron energy was evaluated, which is shown in Fig. 5, where the solid and dashed lines denote the incoming and outgoing energy fluxes, respectively, i.e. the solid line means the de-excitation and the dashed line represents the excitation. Also in Fig. 5 $j\rightarrow k$ denotes the transition from the jth level to the kth level, and j and k are the j-numbers given in Table 1. In the whole range the energy flux due to the de-excitation from $2s^3S$ to the ground state and the recombination are dominant. In a small distance downstream of the sonic point the excitation from $2s^3S$ to $2p^3P$ appears. With the exception of this excitation the collisional transitions are all de-excitations. The electron temperatures and densities have been also obtained in the present calculations. In both cases the electron temperature was found to follow the variation of the heavy-particle temperature. Since the mass of the helium atom is the smallest next to hydrogen, the energy transfer rate due to elastic collision is not negligible in the electron

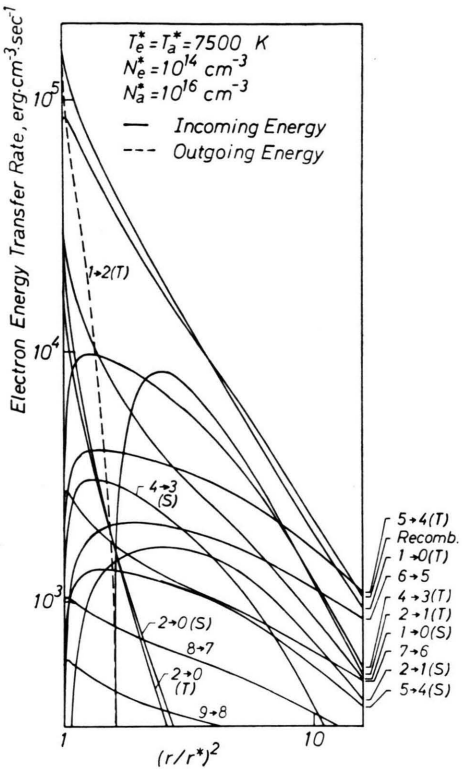

Fig. 5. Electron energy transfer rate due to inelastic collisions for Case I.

energy equation. Due to this strong coupling the electron gas expands with temperatures close to the heavy particle temperatures. When applying the present calculations to ionized gases with heavier atoms, larger differences between the electron and heavy particle temperatures should be observed. According to our calculations the electron density decreases isentropically during the expansion. In the case of the higher electron density the degree of ionization varies from 10^{-2} at the initial point to 9.98×10^{-3} at $r/r^* = 3.67$. Hence one may say that the recombination is frozen in the source flow expansion.

VI. Concluding Remarks

The behaviour of the populations of electronically excited levels in the source flow expansion has been investigated for the case of helium. It was found that the populations of $2s^3S$, $2s^1S$, $2p^3P$ and $2p^1P$ deviated surprisingly from those of the steady state. In addition, in the case of the lower electron density ($N_e^* = 10^{13}$ cm^{-3}) such deviations were appreciable even for the higher levels. From the calculated results we can conclude that the influence of the flow expansion on the population behaviour cannot be neglected and that the steady state model is not practical, especially for lower levels.

In the present conditions of electron temperature and density the difference between the electron and atom temperatures was quite small due to the small mass of helium. If the calculations were applied to heavier atoms, larger temperature differences would have to be expected.

Acknowledgement

The author wishes to express his deep gratitude to Prof. H. Grönig for helpful discussions and valuable suggestions for improvement of the paper.

This work was completed within the term of the fellowship of the Alexander von Humboldt-Stiftung. The author also thanks to the Alexander von Humboldt-Stiftung.

[1] P. Hoffmann and W. L. Bohn, Z. Naturforsch. **22 a**, 1953 [1967].
[2] P. Hoffmann and W. L. Bohn, Kolloquium Plasmatechnik, Jülich, 285 (1972).
[3] S. W. Bowen and C. Park, AIAA J. **9**, 493 [1971].
[4] C. Park, J. Plasma Phys. **9**, 187 [1973].
[5] C. Park, J. Plasma Phys. **9**, 217 [1973].
[6] D. D. McGregor and M. Mitchner, Phys. Fluids **17**, 2155 [1974].
[7] H. Ashkenas and F. S. Sherman, Rarefied Gas Dynamics Vol. II, Toronto, Canada, 84 (1965).
[8] H. W. Drawin and F. Emard, Phys. Letter **43 A**, 333 [1973].
[9] Y. M. Kogan, R. I. Lyagushchenko, and A. D. Khakhaev, Opt. Spectrsc. **15**, 5 [1963].
[10] H. Shirai and K. Tabei, Phys. Rev. **A 7**, 1402 [1973].
[11] F. Roben, W. B. Kunkel, and L. Talbot, Phys. Rev. **132**, 2363 [1963].
[12] H. W. Drawin and F. Emard, EUR-CEA-FC-534, Fontenay-aux-Roses, French 1970.
[13] E. Hinnov and J. G. Hirschberg, Phys. Rev. **125**, 795 [1962].
[14] W. L. Wiese, M. W. Smith, and B. M. Glennon, NSRDS-NBS 4, Washington, USA 1967.
[15] C. H. Kruger and M. Mitchner, Phys. Fluids **10**, 1953 [1967].